

# Dynamical effects of QCD in $q^2\bar{q}^2$ systems

M. Imran Jamil <sup>\*</sup>; Bilal Masud <sup>†</sup>

*Centre For High Energy Physics, Punjab University, Lahore-54590, Pakistan.*

## Abstract

We study the coupling of a tetraquark system to an exchanged meson-meson channel, using a pure gluonic theory based four-quark potential *matrix* model which is known to fit well a large number of data points for lattice simulations of different geometries of a four-quark system. We find that if this minimal-area-based potential matrix replaces the earlier used simple Gaussian form for the gluon field overlap factor  $f$  in its off-diagonal terms, the resulting  $T$ -matrix and phase shifts develop an angle dependence whose partial wave analysis reveals  $D$  wave and higher angular momentum components in it. In addition to the obvious implications of this result for the meson-meson scattering, this new feature indicates the possibility of orbital excitations influencing properties of meson-meson molecules through a polarization potential. We have used a formalism of the resonating group method, treated kinetic energy and overlap matrices on model of the potential matrix, but decoupled the resulting complicated integral equations through the Born approximation. In this exploratory study we have used a quadratic confinement and not included the spin-dependence; we also used the approximation of equal constituent quark masses.

## 1 Introduction

Models of hadronic physics are to be compared with experimental results as well as with our understanding of QCD for large momentum transfers *and* for low momentum transfers where Feynman diagrams are not useful. In this way, models may help us in improving our knowledge of QCD for low and intermediate energies of interest to hadronic spectroscopy and eventually nuclear physics. One way to get this understanding is to note some features present in the perturbative QCD, lattice gauge theory or models of atomic and nuclear physics and check if these features can be used in the low and intermediate energy hadronic physics.

One such feature is an approach based on pair-wise interaction for an interacting multiparticle system (composed of more than two or three particles). This has been successful in atomic and many-nucleon systems; the corresponding two-body interaction being described by Coulombic and Yukawa potential, for example. The question is if the explicit presence of *Non-Abelian* gluon field can also be replaced by *two body* interquark potentials. The simplest way to use such a model is to try a *sum* of two-body potentials or interactions, the usual approach of atomic and nuclear physics. For comparison, it can be noted that the lowest order perturbative Feynman diagrams amplitudes are of this form, and a simple extension of this diagrammatic approach to multi-quarks also has this pattern; see ref. [1], and the later ones in the same approach, where the one gluon exchange potential, though, is replaced by Coulombic-plus-linear-plus-hyperfine. If the numerically calculated energies of the four-quark systems on a lattice, in the static quark limit, are compared with a model that use only a *sum* of two-quark potentials, the model give a gross overestimate of the (magnitude of) four-quark binding energies; see fig. 4 of the same ref.[2]. A gluon field overlap factor  $f$  was introduced [3] essentially as a solution to this discrepancy. This factor multiplied only off-diagonal elements of the overlap, kinetic and potential energy matrices of the otherwise pairwise-sum-based Hamiltonian in the three-dimensional basis of the model system of four valence quarks/antiquarks and the purely gluonic field between them. Initially [3] the geometrical dependence of  $f$  on the quark positions was chosen purely based on computational convenience and had no known comparison with any QCD simulations. But when its different forms were compared [4] with

---

<sup>\*</sup>e mail: mimranjamil@hotmail.com

<sup>†</sup>e mail: bilalmasud@chep.pu.edu.pk

two-colour lattice numerical simulations in the pure gluonic theory, a factor of  $\exp(-kS_{min})$  had to be included in off-diagonal terms of the every version of the potential and overlap matrices;  $S_{min}$  is the minimal spatial area bounded by four external lines joining the four quarks and  $k$  is geometrically a constant. Only this way, a version of the model was eventually able to fit well "100 pieces of data—the ground and first excited states of configurations from six (kinds of) different four-quark geometries (including squares, rectangles, quadrilaterals and tetrahedra) calculated on a  $16^3 \times 32$  lattice—with only four independent parameters to describe the interactions connecting the basis states". It is to be noted that this exponential dependence on the spatial area in the model can be possibly traced back to the related use of the space-time area in more familiar models of Wilson loops studying time evolutions of a quark-antiquark pair. The connection was first suggested by a Wilson loop matrix in a strong coupling expansion scheme (see figs. 4 and 5 of ref.[5]) and appeared in above mentioned model [4] of the numerically evaluated Wilson loop matrix of the  $SU(2)_c$  simulations. A full  $SU(3)_c$  simulation [6] performed a bit later again showed the need for  $f$  model, though detailed geometrical dependence of  $f$  could not be studied in this 3 colour lattice gauge study. But a later numerical lattice study [7] by a reputed group of the *full*  $2 \times 2$  matrix of the Wilson loops correlators and of "the interaction energy of the confining strings in the static rectangular tetraquark system in  $SU(3)$  gluodynamics" was well modeled again by a surface model, namely their *soap film* model that also incorporates (a flip to) the multi  $Y$  type linear potential emerging from recent numerical simulations [8]. The basis state overlap  $g$  [7] in the soap film model has a role similar to the gluon field overlap factor  $f$  of ref.[4]; both  $f$  and  $g$  appear only in the off-diagonal terms of the respective matrices ( $N$  and  $T$ ) of overlaps of the basis states. Continuing on the spatial and space-time areas, it can be pointed out that both kind of areas appear in eq.(13) of the ref.[7] and are related to Wilson loops as earlier eq.(12) there indicates.

Actually, above are models of the matrices of pure gluonic theory Wilson loops. The diagonal terms in these matrices are time evolutions of a tetraquark clustering and off-diagonal terms [5, 7] are for time evolution that start from one tetraquark clustering (or topology) and end at another one. The numerical evaluation of the off-diagonal Wilson loops has been perhaps done in refs. [4] (and previous ones by the same group) and [7] only. But the diagonal Wilson loops have been studied by many other groups, most familiar being the studies reported in ref.[8] and the previous works by the same group. For one set of quark configurations, the diagonal studies are limited to only one Wilson loop. In a sense, this means limitation to only one state of the gluonic field as well, namely the one with the least energy *to which* system flips; if there are other states mentioned in the literature, these are either for comparison purpose (*from which* the system flips) or the excited state "contaminations". But a general study should *actually* incorporate a variety of basis states and thus include off-diagonal Wilson loops *as well*. The spatial area we are working on appears only in the off-diagonal Wilson loops and thus our work is not to be confused with the usual study of the diagonal Wilson loops effects. It is to be admitted that works like ref.[8] have indicated improvements in both evaluations and models of the diagonal Wilson loops and we have not included these improvements in our model of the diagonal term. But this is not a serious flaw, as a dynamical study [9] using these improved diagonal models mentions in its conclusions and comments that the "dynamics of (tetraquark) binding is dominated by the simple flip-flop term", meaning that the essentially new connected string (butterfly) term introduced through the work of ref.[8] is dynamically "not rewarding". It is to be noted that our diagonal terms include both terms whose minimum is the flip-flop term.

This advocates the  $\exp(-kS)$  form of  $f$  for static two quarks and two antiquarks. For a comparison with actual (hadron) experiments, we have to incorporate quark motion as well, possibly through using quark wave functions. The resulting four-body Schrödinger equation can be solved, as in ref. [10], variationally for the ground state of the system and the effective meson-meson potentials. Alternatively, the Hamiltonian emerging from the  $q^2\bar{q}^2$  model has been diagonalized in the simple harmonic oscillator basis [11], or was sandwiched between the external meson wave functions to give a transition amplitude of the *Born diagrams* [1, 12] that is related to meson-meson phase shifts. We have used a formalism (resonating group method [13]) that was, for the  $q^2\bar{q}^2$  system, originally [3] used in a way that allowed finding *inter-meson* dependence with the dependence on a quark-antiquark distance being pre-fixed. The formalism allows using the best available knowledge of a meson wave function, though a simple Gaussian form for the wave functions and correspondingly a quadratic quark-antiquark potential was used for computational convenience. We have used this same formalism that can be generalized to using realistic meson wave functions and finding the inter-cluster dependence. But because of the additional computational problems due to a totally non-separable exponential of (a negative constant times) area in  $f$ , presently we had to also pre-specify a plane-wave form of the inter-cluster dependence along with

still using Gaussian wave functions; effectively this means using a Born approximation as well. We have pointed out, though, that these wave function approximations are better than what their naive impression conveys: The Gaussian dependence on the quark-antiquark distance has the potential of resembling the realistic meson wave functions through an adjustment of its parameters [14]. And the plane wave form of the inter-cluster dependence is justified through a feeble inter-cluster (meson-meson) interaction noted in previous works [10, 3, 1]; the meson-meson phase shifts resulting from this work are also much less than a radian. *Only by using the Born-approximation*, the resulting coupled integral equations for inter-cluster wave functions could be decoupled in this work. This decoupling allowed us to numerically calculate the off-diagonal elements as nine-dimensional integrals for the components of the eventual four position 3-vectors; only the overall center-of-mass dependence could be analytically dealt with in a trivial manner. Before this numerical integration, for the kinetic energy terms we had to differentiate the area in  $f$ . The form of area used in the detailed form of the  $Q^2\bar{Q}^2$  model, that we take from ref. [4], has square roots of the functions of our position variables. Thus a differentiation of this area form yields in denominators combinations of position variables that become zero somewhere in the ranges of integrations to be later done. The numerical evaluations of the resulting nine-dimensional improper integrals is expected to be too demanding, as our initial explorations indicated. Thus, for the to-be-differentiated right  $\sqrt{f}$  part of the some kinetic energy terms we replaced the area by an approximated quadratic form whose differentiation does not result in negative powers of the position variables.

We also find that the use of the  $f$  factor in the new form reduces the long range meson-meson interaction and thus as usual solves the well known Van der Walls force problem [15, 9] with the otherwise naive sum of one gluon exchange pair-wise interaction. It has been said [10] that dynamically it is not a serious problem because of the quark-antiquark pair creation and because of the wave function damping of the large distance configurations. Though ref. [6] partly incorporated both the quark-antiquark pair creation and the meson wave functions and still showed a need for the  $f$  factor, through the present work we want to point out that the dynamical role of the  $f$  factor in meson-meson interactions is *not limited* to solving Van der Walls force problem or pointing out [16] otherwise over-binding in certain meson-meson systems. The  $f$  factor points certain features (non-separability of  $f$ ) of QCD that are 1) indicated by lattice simulations and 2) can be compared with actual experiments.

There have been recent hadron-level studies [17][9] using the above mentioned improved models of the diagonal Wilson loops. But the quark level limitations of the models [18][8] mean similar limitations for the hadron-level results: [17][9] study the properties (like binding energy and *direct potential* [19]) of the ground state itself (or in isolation), whereas we aim to study the dynamical coupling of a tetraquark state to other basis state(s) of the tetraquark system—essentially to the other clustering or the exchanged channel. Thus, as we say in the abstract, in addition to doing the phase-shift calculations for a meson-meson scattering, we study a coupling that can affect even the ground state itself through a second order perturbation theory effect named polarization potential [19]. That is, after including the quark mass differences, a meson-meson state may not be degenerate with an exchanged channel and thus the coupling between this state and the exchanged intermediate one (a hadron loop) may help resolve the underlying structure of a possible meson-meson state. Such a state may be a meson-meson molecule that can be formed by the ground state. This also makes a study of the dynamical coupling of a meson-meson channel to exchanged one worth pursuing.

In section 2 we have written the total state vector of the  $q^2\bar{q}^2$  system as in RGM, along with introducing the Hamiltonian  $H$  of the system without the  $f$  factor and then modifying  $H$  through the  $f$ . In section 3 different position dependent forms of  $f$  have been described, including the approximate forms that we had to use. In section 4 we have solved the integral equations for a meson meson molecule in the absence of spin degrees of freedom and with all equal quark masses. This section ends with a prescription to find the phase shifts. In the last section we have presented the numerical values of the phase shifts for different forms of  $f$ , for different values of free parameter  $k_f$  and for different values of angle  $\theta$  between  $\mathbf{P}_1$  and  $\mathbf{P}_2$ .

## 2 The $Q^2\bar{Q}^2$ Hamiltonian and the wave-function

Using adiabatic approximation we can write the total state vector of a system containing two quarks two antiquarks and the gluonic field between them as a sum of the product of the quarks ( $Q$  or  $\bar{Q}$ ) position dependent function  $\Psi_g(\mathbf{r}_1, \mathbf{r}_2, \mathbf{r}_3, \mathbf{r}_4)$  and the gluonic field state  $|k\rangle_g$ .  $|k\rangle_g$  is defined as a state which approaches  $|k\rangle_c$  in the weak coupling limit, with  $|1\rangle_c = |1_{\bar{3}}1_{24}\rangle_c$ ,  $|2\rangle_c = |1_{14}1_{23}\rangle_c$  and  $|3\rangle_c = |\bar{3}_{12}3_{34}\rangle_c$ .

In lattice simulations of the corresponding (gluonic) Wilson loops it is found that the lowest eigenvalue of the Wilson matrix, that is energy of the lowest state, is always the same for both  $2 \times 2$  and  $3 \times 3$  matrices provided that  $|1\rangle_g$  or  $|2\rangle_g$  has the lowest energy [4]. The later calculations [7] of the tetraquark system were also done with a two level approximation. Taking advantage of these observations, we have included in our expansion only two basis states. As in resonating group method,  $\Psi_g(\mathbf{r}_1, \mathbf{r}_2, \mathbf{r}_3, \mathbf{r}_4)$  or  $\Psi_g(\mathbf{R}_c, \mathbf{R}_k, \mathbf{y}_k, \mathbf{z}_k)$  is written as product of known dependence on  $\mathbf{R}_c, \mathbf{y}_k, \mathbf{z}_k$  and unknown dependence on  $\mathbf{R}_k$ . i.e.  $\Psi_g(\mathbf{r}_1, \mathbf{r}_2, \mathbf{r}_3, \mathbf{r}_4) = \Psi_c(\mathbf{R}_c)\chi_k(\mathbf{R}_k)\psi_k(\mathbf{y}_k, \mathbf{z}_k)$ . Here  $\mathbf{R}_c$  is the center of mass coordinate of the whole system,  $\mathbf{R}_1$  is the vector joining the center of mass of the clusters  $(1, \bar{3})$  and  $(2, \bar{4})$ ,  $\mathbf{y}_1$  is the position vector of quark 1 with respect to  $\bar{3}$  within the cluster  $(1, \bar{3})$  and  $\mathbf{z}_1$  is the position vector of quark 2 with respect to  $\bar{4}$  within the cluster  $(2, \bar{4})$ . The same applies to  $\mathbf{R}_2, \mathbf{y}_2$  and  $\mathbf{z}_2$  for the clusters  $(1, \bar{4})$  and  $(2, \bar{3})$ . Similarly we can define  $\mathbf{R}_3, \mathbf{y}_3$  and  $\mathbf{z}_3$  for the clusters  $(1, 2)$  and  $(\bar{3}, \bar{4})$ . Or we can write them in terms of position vector of the four particles (quarks or antiquarks) as follow

$$\mathbf{R}_1 = \frac{1}{2}(\mathbf{r}_1 + \mathbf{r}_{\bar{3}} - \mathbf{r}_2 - \mathbf{r}_{\bar{4}}), \mathbf{y}_1 = \mathbf{r}_1 - \mathbf{r}_{\bar{3}} \text{ and } \mathbf{z}_1 = \mathbf{r}_2 - \mathbf{r}_{\bar{4}}, \quad (1)$$

$$\mathbf{R}_2 = \frac{1}{2}(\mathbf{r}_1 + \mathbf{r}_{\bar{4}} - \mathbf{r}_2 - \mathbf{r}_{\bar{3}}), \mathbf{y}_2 = \mathbf{r}_1 - \mathbf{r}_{\bar{4}} \text{ and } \mathbf{z}_2 = \mathbf{r}_2 - \mathbf{r}_{\bar{3}} \quad (2)$$

and

$$\mathbf{R}_3 = \frac{1}{2}(\mathbf{r}_1 + \mathbf{r}_2 - \mathbf{r}_{\bar{3}} - \mathbf{r}_{\bar{4}}), \mathbf{y}_3 = \mathbf{r}_1 - \mathbf{r}_2 \text{ and } \mathbf{z}_3 = \mathbf{r}_{\bar{3}} - \mathbf{r}_{\bar{4}}. \quad (3)$$

Thus meson meson state vector in the restricted gluonic basis is written as

$$|\Psi(\mathbf{r}_1, \mathbf{r}_2, \mathbf{r}_3, \mathbf{r}_4; g)\rangle = \sum_{k=1}^2 |k\rangle_g \Psi_c(\mathbf{R}_c)\chi_k(\mathbf{R}_k)\xi_k(\mathbf{y}_k)\zeta_k(\mathbf{z}_k). \quad (4)$$

Here  $\xi_k(\mathbf{y}_k) = \frac{1}{(2\pi d^2)^{\frac{3}{4}}} \exp(\frac{-\mathbf{y}_k^2}{4d^2})$  and  $\zeta_k(\mathbf{z}_k) = \frac{1}{(2\pi d^2)^{\frac{3}{4}}} \exp(\frac{-\mathbf{z}_k^2}{4d^2})$ . These Gaussian forms of meson wave functions are, strictly speaking, the wave functions of a quadratic confining potential. But, as pointed out in text below fig. 1 of ref. [14], the overlap of a Gaussian wave function and the eigenfunction of the realistic linear plus colombic potential can be made as close as 99.4% by properly adjusting its parameter  $d$ . A realistic value of  $d$  mimicking a realistic meson wave function depends on the chosen scattering mesons and thus is postponed to our future work [20]. Presently, to explore the qualitative implications of the geometric features of the gluonic overlap factor  $f$ , we have used in  $\xi_k(\mathbf{y}_k)$  and  $\zeta_k(\mathbf{z}_k)$  a value  $d = 0.558$  fm defined by the relation  $d^2 = \sqrt{3}R_c^2/2$  [16], with  $R_c = 0.6$  fm being the r.m.s. charge radius of the qq system whose wave function is derived by using the same quadratic confining potential.

As for the Hamiltonian, for  $f=1$  the total Hamiltonian  $H$  of our 4-particle system is taken as [21]

$$\hat{H} = \sum_{i=1}^{\bar{4}} \left[ m_i + \frac{\hat{P}_i^2}{2m_i} \right] + \sum_{i < j}^{\bar{4}} v(\mathbf{r}_{ij}) \mathbf{F}_i \cdot \mathbf{F}_j. \quad (5)$$

Our same constituent quark mass value  $m = 0.3\text{GeV}$  for all quarks and antiquarks is one used in refs. [3], and our kinetic energy operator is similarly non-relativistic; it is included in our aims to compare with this work and isolate the effects only due to a different expression for the  $f$ . In above each of  $\mathbf{F}_i$  has 8 components  $F_i^l = \lambda^l/2$ ,  $l = 1, 2, 3, \dots, 8$  and  $F_i^{l*} = \lambda^{l*}/2$ ,  $\lambda^l$  are Gell-Mann matrices operating on the  $i$ -th particle;  $l$  is shown as a superscript only to avoid any possible confusion with subscript  $i$  which labels a particle.

For the pairwise  $q\bar{q}$  potential, we have used a quadratic confinement

$$v_{ij} = Cr_{ij}^2 + \bar{C} \text{ with } i, j = 1, 2, \bar{3}, \bar{4}. \quad (6)$$

for exploratory study. While we have neglected short range coulomb like interactions as well as spin-dependent terms. Along with that non relativistic limit has also been taken. The model used by Vijande [9] is also restricted to these limits. As for the within-a-cluster dependence of the wave function, this use of the quadratic potential in place of the realistic Coulombic plus linear may change the full wave function. In the within-a-cluster, this change of wave function is found to result in a change of an overlap integral from 100% to 99.4% only provided the parameter  $d$  of the wave function is adjusted. Although the expression for  $P_c$  written immediately after eq.(26) suggests a way to connect the additional parameter of

the full wave function with that of a cluster, it is difficult to make a similar overlap test for the full wave function. But there is no a priori reason to deny that at least the qualitative features (like a new kind of angle dependence mentioned in the results part) we want to point out using this quadratic confinement would survive in a more realistic calculation; a similar exploration of the  $q^2\bar{q}^2$  system properties was first done [10] using a quadratic confinement and later extended and improved calculation [21] with more realistic pair-wise interaction reinforced the  $K\bar{K}$  results obtained initially through the quadratic confinement. It seems that a proper adjustment the parameters of the quadratic (or SHO) model can reasonably simulate a  $q\bar{q}$  or even a  $q^2\bar{q}^2$  system. In our case, this adjustment of the parameters can be done once a choice of actual scattering mesons is made in a formalism [20] that incorporates spin and flavour degrees of freedom. But, as shown in fig. 2(b) of ref.[10], properties of the  $q^2\bar{q}^2$  system may not be very sensitive to the actual values of the parameters and we expect our presently chosen values of the parameters to well indicate the essential features resulting from the non-separable form of the gluonic field overlap factor  $f$ .

For the central simple harmonic oscillator potential of eq.(6), the above mentioned size  $d$  in the eigenfunctions  $\xi_k(\mathbf{y}_k)$  and  $\zeta_k(\mathbf{z}_k)$  is related to the quadratic coefficient  $C$  which thus is given a value of  $-0.0097\text{GeV}^3$ .

As in a resonating group calculation, we take only variations in the  $\chi_k$  factor of the total state vector of the system written in eq.(4). Setting the coefficients of linearly independent arbitrary variations  $\delta\chi_k(\mathbf{R}_k)$  as zero and integrating out  $R_c$ ,  $\langle\delta\psi | H - E_c | \psi\rangle = 0$  from eq.(4) gives

$$\sum_{l=1}^2 \int d^3y_k d^3z_k \xi_k(\mathbf{y}_k) \zeta_k(\mathbf{z}_k)_g \langle k | H - E_c | l \rangle_g \chi_l(\mathbf{R}_l) \xi_l(\mathbf{y}_l) \zeta_l(\mathbf{z}_l) = 0, \quad (7)$$

for each of the  $k$  values (1 and 2). According to the (2 dimensional basis) model  $I_a$  of ref. [4], the normalization, potential energy and kinetic energy matrices in the corresponding gluonic basis are

$$N = \begin{pmatrix} 1 & \frac{1}{3}f \\ \frac{1}{3}f & 1 \end{pmatrix}, \quad (8)$$

$$V = \begin{pmatrix} \frac{-4}{3}(v_{1\bar{3}} + v_{2\bar{4}}) & \frac{4}{9}f(v_{12} + v_{3\bar{4}} - v_{1\bar{3}} - v_{2\bar{4}} - v_{1\bar{4}} - v_{2\bar{3}}) \\ \frac{4}{9}f(v_{12} + v_{3\bar{4}} - v_{1\bar{3}} - v_{2\bar{4}} - v_{1\bar{4}} - v_{2\bar{3}}) & \frac{-4}{3}(v_{1\bar{4}} + v_{2\bar{3}}) \end{pmatrix} \quad (9)$$

and

$${}_g\langle k | K | l \rangle_g = N(f)_{k,l}^{\frac{1}{2}} \left( \sum_{i=1}^4 -\frac{\nabla_i^2}{2m} \right) N(f)_{k,l}^{\frac{1}{2}}. \quad (10)$$

This is the modification, through the  $f$  factor, to the Hamiltonian as much as we need it for the integral equations below in section 4 (that is only the modified matrix elements).

### 3 Different forms of $f$

Ref. [4] supports through a comparison with numerical lattice simulations a form of  $f$  that was earlier [15] suggested through a quark-string model extracted from the strong coupling lattice Hamiltonian gauge theory. This is

$$f = \exp(-b_s k_f S), \quad (11)$$

$S$  being the area of minimal surface bounded by external lines joining the position of the two quarks and two antiquarks, and  $b_s = 0.18\text{GeV}^2$  is the standard string tension [22, 18],  $k_f$  is a dimensionless parameter whose value of 0.57 was decided in ref. [4] by a fit of the simplest two-state area-based model (termed model Ia) to the numerical results for a selection of  $Q^2\bar{Q}^2$  geometries. It is shown there [4] that the parameters, including  $k_f$ , extracted at this  $SU(2)_c$  lattice simulation with  $\beta = 2.4$  can be used directly in, for example, a resonating group calculation of a four quark model as the continuum limit is achieved for this value of  $\beta$ .

The simulations reported in ref. [4] were done in the 2-colour approximation. But, for calculating the dynamical effects, we use actual  $SU(3)$  colour matrix elements of ref. [3]. The only information we take from the computer simulations of ref. [4] is value of  $k_f$ . This describes a geometrical property of the gluonic field (its spatial rate of decrease to zero) and it may be the case that the geometrical properties

of the gluonic field are not much different for different number of colours, as suggested for example by successes of the geometrical flux tube model. Situation is more clear, though, for the mass spectra and the string tension generated by the gluonic field: ref. [23] compare these quantities for  $SU(2)_c$ ,  $SU(3)_c$  and  $SU(4)_c$  gauge theories in 2+1 dimensions and find that the ratio of masses are, to a first approximation, are independent of the number of colours. Their preliminary calculations in 3+1 dimensions indicate a similar trend. Directly for the parameter  $k_f$ , appearing in the overlap factor  $f$  studied in this work, the similar conclusion can be drawn from a comparison of the mentioned lattice calculations [6] on the interaction energy of the two heavy-light  $Q^2\bar{q}^2$  mesons in the realistic  $SU(3)_c$  gauge theory with ref. [4] that uses  $SU(2)_c$ . For interpreting the results in terms of the potential for the corresponding single heavy-light meson ( $Q\bar{q}$ ), a Gaussian form

$$f = \exp(-b_s k_f \sum_{i < j} r_{ij}^2) \quad (12)$$

of the gluonic field overlap factor  $f$  is used in this ref. [6] for numerical convenience and not the minimal area form. But for a particular geometry, the two exponents (the minimal area and the sum of squared distances) in these two forms of  $f$  are related and thus for a particular geometry a comparison of the parameter  $k_f$  multiplying area and corresponding (different!)  $k_f$  multiplying sum of squares in eq. (14) of ref. [6] is possible. We note that, after correcting for a ratio of 8 between the sum of distance squares (including two diagonals) and the area for the square geometry, the colour-number-generated relative difference for this geometry is just 5%: the coefficient is  $0.075 \times 8 = 0.6$  multiplying sum of squared distances and 0.57 multiplying the minimal area. But, as the precise form of  $f$  is still under development (the latest work [7] has covered only a very limited selection of the positions of tetraquark constituents) and the expression for the area in its exponent needs improvement, it is not sure precisely what value of the  $k_f$  best simulates QCD and we have mainly worked with an approximate value of 0.5 that is also mentioned in ref.[4] and is numerically easier to deal with. (It is to be noted that the soap film model of ref.[7] does not treat  $k_f$  as a variational parameter. If that is interpreted as fixing  $k_f$  at 1, this prescription might have been successful due to their selection of quark configurations being limited to planar ones; a work [24] by UKQCD that is limited to planar geometries also favors a value closer to 1. But their more general work [4] resulted in a value of  $k_f$  near 0.5.)

For the area as well, ref. [4] used an approximation: A good model of area of the minimal surface could be that given in ref. [25] as

$$S = \int_0^1 du \int_0^1 dv |(u\mathbf{r}_{1\bar{3}} + (1-u)\mathbf{r}_{\bar{4}2}) \times (v\mathbf{r}_{2\bar{3}} + (1-v)\mathbf{r}_{\bar{4}1})| \quad (13)$$

(Work is in progress [26], to judge the surface used in this model, and its area, from the point of differential geometry and there are indications that this is quite close to a minimal surface.) But the simulations reported in ref. [4] were carried out for the  $S$  in eq.(11) being "the average of the sum of the four triangular areas defined by the positions of the four quarks". Although for the tetrahedral geometry the  $S$  used in ref. [4] is as much as 26 percent larger than the corresponding minimal-like area of ref. [25], it can be expected that their fitted value of  $k_f$  is reduced to partially compensate this over estimate of the  $S$  area. Anyway, as we are calculating the dynamical effects of the model of ref. [4], we have used the form of  $S$  that is used in this work.

The area  $S$  of ref. [4] becomes (with a slight renaming)

$$S = \frac{1}{2}[S(134) + S(234) + S(123) + S(124)], \quad (14)$$

where  $S(ijk)$  is the area of the triangle joining the vertices of the positions of the quarks labeled as  $i, j$  and  $k$ . In the notation of eqs.(1-3) this becomes  $S(134) = \frac{1}{2}|\mathbf{y}_1 \times \mathbf{z}_3| = \frac{1}{2}|(\mathbf{R}_2 + \mathbf{R}_3) \times (\mathbf{R}_1 - \mathbf{R}_2)|$ ,  $S(234) = \frac{1}{2}|\mathbf{z}_2 \times \mathbf{z}_3| = \frac{1}{2}|(\mathbf{R}_3 - \mathbf{R}_1) \times (\mathbf{R}_1 - \mathbf{R}_2)|$ ,  $S(123) = \frac{1}{2}|\mathbf{y}_3 \times \mathbf{z}_2| = \frac{1}{2}|(\mathbf{R}_1 + \mathbf{R}_2) \times (\mathbf{R}_3 - \mathbf{R}_1)|$  and  $S(124) = \frac{1}{2}|\mathbf{y}_3 \times \mathbf{z}_1| = \frac{1}{2}|(\mathbf{R}_1 + \mathbf{R}_2) \times (\mathbf{R}_3 - \mathbf{R}_2)|$ . Written in terms of the rectangular components

$(x_1, y_1, z_1)$  of  $\mathbf{R}_1$ ,  $(x_2, y_2, z_2)$  of  $\mathbf{R}_2$  and  $(x_3, y_3, z_3)$  of  $\mathbf{R}_3$ , we have

$$S(134) = \frac{1}{2} \left\{ \begin{aligned} & \left( x_2^2 + y_2^2 + z_2^2 + 2(x_2x_3 + y_2y_3 + z_2z_3) + x_3^2 + y_3^2 + z_3^2 \right) \\ & \left( x_1^2 + y_1^2 + z_1^2 - 2(x_1x_2 + y_1y_2 + z_1z_2) + x_2^2 + y_2^2 + z_2^2 \right) \\ & - \left( x_1x_2 + y_1y_2 + z_1z_2 - (x_2^2 + y_2^2 + z_2^2) + x_1x_3 + y_1y_3 + z_1z_3 - (x_2x_3 + y_2y_3 + z_2z_3) \right)^2 \end{aligned} \right\}^{\frac{1}{2}}. \quad (15)$$

Explicit rectangular expressions for  $S(234)$ ,  $S(123)$  and  $S(124)$  are similar.

This form of  $S$  has square roots. For the  $K.E.$  part of the Hamiltonian matrix (see eq.(10) ), we have to differentiate an exponential of this square root. After differentiating we can have negative powers of  $S$  and when they will be integrated in the latter stages can have singularities in the integrands resulting in computationally too demanding nine-dimensional improper integrals. Thus we have availed to ourselves an approximated  $S$ , named  $S_a$ , which is a sum of different quadratic combinations of quarks positions. We chose  $S_a$  by minimizing  $\int d^3R_1 d^3R_2 d^3R_3 (S - S_a)^2$  with respect to the coefficients of the quadratic position combinations; that is, these coefficients are treated as variational parameters. The first (successful) form which we tried for  $S_a$  was

$$S_a = a(x_1^2 + y_1^2 + z_1^2) + b(x_2^2 + y_2^2 + z_2^2) + c(x_3^2 + y_3^2 + z_3^2) + d x_1 x_2 + e y_1 y_2 + f z_1 z_2 + g x_2 x_3 + h y_2 y_3 + i z_2 z_3 + j x_1 x_3 + k y_1 y_3 + l z_1 z_3. \quad (16)$$

This contained 12 variational parameters a,b,c,...,l. Minimization gave values (reported with accuracy 4 though in the computer program accuracy 16 was used)as

$$a = 0.4065, b = 0.4050, c = 0.3931, j = -0.0002, l = -0.0002.$$

In the reported accuracy other parameters are zero. Here limits of integration were from -15 to 15 in  $\text{GeV}^{-1}$ . We also tried  $S_a$  as

$$\sum_{i=1}^3 a_i(x_i^2 + y_i^2 + z_i^2) + \sum_{i,j=1}^3 (b_{i,j}x_i y_j + c_{i,j}x_i z_j + d_{i,j}y_i z_j) + \sum_{i<j,j=2}^3 (e_{i,j}x_i x_j + f_{i,j}y_i y_j + g_{i,j}z_i z_j)$$

and

$$\sum_{i=1}^3 (l_i x_i^2 + m_i y_i^2 + n_i z_i^2) + \sum_{i,j=1}^3 (b_{i,j}x_i y_j + c_{i,j}x_i z_j + d_{i,j}y_i z_j) + \sum_{i<j,j=2}^3 (e_{i,j}x_i x_j + f_{i,j}y_i y_j + g_{i,j}z_i z_j),$$

with variational parameters being 39 and 45 respectively. Both the latter forms gave the same result as we got with 12 variational parameters, and hence this 12 parameter form was used in the section below. This form gives dimensionless standard-deviation, defined as

$$\sqrt{\frac{\langle (S - S_a)^2 \rangle - (\langle S - S_a \rangle)^2}{\langle S^2 \rangle}},$$

being approximately equal to 21% . Here,

$$\langle X \rangle = \frac{\int (X) d^3R_1 d^3R_2 d^3R_3}{\int (1) d^3R_1 d^3R_2 d^3R_3}.$$

As this is not too small, in our main calculations we have made a minimal use of this further approximated area  $S_a$  (only for the to-be-differentiated right  $\sqrt{F}$  part (see eq.10 ) of the kinetic energy term and here only for derivatives of the exponent).

## 4 Solving the integral equations

In eq.(7) for  $k = l = 1$  (a diagonal term), we used the linear independence of  $\mathbf{y}_1$ ,  $\mathbf{z}_1$  and  $\mathbf{R}_1$  (see eq.(1)) to take  $\chi_1(\mathbf{R}_1)$  outside the integrations w.r.t.  $\mathbf{y}_1$  and  $\mathbf{z}_1$ . For the off-diagonal term with  $k = 1$  and  $l = 2$  we replaced  $\mathbf{y}_1$  and  $\mathbf{z}_1$  with  $\mathbf{R}_2$  and  $\mathbf{R}_3$ , with Jacobian of transformation as 8. For regulating the space derivatives of the exponent of  $f$  (see the three sentences immediately following eq.(15) above) we temporarily replaced  $S$  in it by its quadratic approximation  $S_a$ . As a result, we obtained the following equation:

$$\begin{aligned} & \left( \frac{3\omega}{2} - \frac{1}{2\mu_{12}} \nabla_{R_1}^2 + 24C_o d^2 - \frac{8}{3} \bar{C} - E_c + 4m \right) \chi_1(\mathbf{R}_1) \\ & + \int d^3 R_2 d^3 R_3 \exp\left(-b_s k_f S\right) \exp\left(-\frac{R_1^2 + R_2^2 + 2R_3^2}{2d^2}\right) \left[ -\frac{8}{6m(2\pi d^2)^3} g_1 \exp\left(\frac{1}{2} b_s k_f S\right) \right. \\ & \quad \left. \exp\left(-\frac{1}{2} b_s k_f S_a\right) + \frac{32}{9(2\pi d^2)^3} \left(-4CR_3^2 - 2\bar{C}\right) - \frac{8(E_c - 4m)}{3(2\pi d^2)^3} \right] \chi_2(\mathbf{R}_2) = 0, \end{aligned} \quad (17)$$

with, written up to accuracy 4,

$$\begin{aligned} g_1 = & -1.4417 + 0.0258x_1^2 + 0.0258x_2^2 + 0.0254x_3^2 + 0.0258y_1^2 + \\ & 0.0258y_2^2 + 0.0254y_3^2 + 0.0258z_1^2 + 0.0258z_2^2 + 0.0254z_3^2. \end{aligned} \quad (18)$$

For the consistency of  $\xi_k(\mathbf{y}_k)$  and  $\zeta_k(\mathbf{z}_k)$  with eq.(6)  $\omega = 1/md^2 = 0.416\text{GeV}$ . For convenience in notation we take  $C_o = -C/3$ . Here in the first channel for  $k = 1$  the constituent quark masses has been replaced by the reduced mass  $\mu_{12} = M_1 M_2 / (M_1 + M_2)$ , where  $M_1$  and  $M_2$  are masses of hypothetical mesons; a similar replacement has been done in ref.[3].

At this stage we can fit  $\bar{C}$  to a kind of "hadron spectroscopy" for our equal quark mass case:

For the large separation there is no interaction between  $M_1$  and  $M_2$ . So the total center of mass energy in the large separation limit will be the sum of kinetic energy of relative motion and masses of  $M_1$  and  $M_2$  i.e. in the limit  $R_1 \rightarrow \infty$  we have

$$\left[ -\frac{1}{2\mu_{12}} \nabla_{R_1}^2 + M_1 + M_2 \right] \chi_1(\mathbf{R}_1) = E_c \chi_1(\mathbf{R}_1). \quad (19)$$

By comparing, in this limit, eq.(19) and eq.(17) we have  $M_1 + M_2 = 4m + 3\omega - 8\bar{C}/3$ . (A use of the first term of eq.(6) for the colour-basis diagonal matrix element of eq.(5) gives  $-4C/3 = \mu\omega^2/2 = \mu\omega/2md^2$ , giving  $24C_o d^2 = 3\omega/2$  for the reduced mass  $\mu$  of a pair of equal mass quarks being  $m/2$ ; the diagonal elements in any form of the  $f$  model for the gluonic basis are the same as those for the colour basis.) By choosing  $M_1 + M_2 = 3\omega$  we have  $\bar{C} = 3m/2 = 0.45\text{GeV}$ . This choice of the hypothetical meson masses is the one frequently used in ref. [3] for an illustration of the formalism; when we incorporate flavour and spin dependence [20] the same fit, something like in ref. [16], we plan to fit our quark masses to actual meson spectroscopy. We can then choose to fit even the parameter  $C$  or  $C_0$  of our potential model to hadron spectroscopy rather than deciding it, as in ref. [3] and the present work, through a combination of baryon radii and harmonic oscillator model. But we do not see any reason why the qualitative effects (for example, an angle dependance, see the section below) pointed out through the present work should disappear for a phenomenologically explicit case.

Completing our integral equations before finding a solution for two  $\chi$ 's, for  $k = 2$  in eq.(7) we took  $\chi_2(\mathbf{R}_2)$  outside of integration for the diagonal term, for the off-diagonal term we replaced  $\mathbf{y}_2$  and  $\mathbf{z}_2$  by  $\mathbf{R}_1$  and  $\mathbf{R}_3$  and replaced  $S$  by  $S_a$ . This resulted in

$$\begin{aligned} & \left( \frac{3\omega}{2} - \frac{1}{2\mu_{34}} \nabla_{R_2}^2 + 24C_o d^2 - \frac{8}{3} \bar{C} - E_c + 4m \right) \chi_2(\mathbf{R}_2) \\ & + \int d^3 R_1 d^3 R_3 \exp\left(-b_s k_f S\right) \exp\left(-\frac{R_1^2 + R_2^2 + 2R_3^2}{2d^2}\right) \left[ -\frac{8}{6m(2\pi d^2)^3} g_1 \exp\left(\frac{1}{2} b_s k_f S\right) \right. \\ & \quad \left. \exp\left(-\frac{1}{2} b_s k_f S_a\right) + \frac{32}{9(2\pi d^2)^3} \left(-4CR_3^2 - 2\bar{C}\right) - \frac{8(E_c - 4m)}{3(2\pi d^2)^3} \right] \chi_1(\mathbf{R}_1) = 0. \end{aligned} \quad (20)$$



In the 2nd channel, for  $k = 2$ , the constituent quark masses are replaced by the reduced mass  $\mu_{34} = M_3 M_4 / (M_3 + M_4)$ , where  $M_3$  and  $M_4$  are masses of hypothetical mesons.

Now we solve our two integral equations. As our space derivatives have been regularized, we no longer need further-approximated  $S_a$  and we replace this by the original  $S$  in eq.(20). Below we take Fourier transform of eq.(17). This gives us a nine dimensional integral of, amongst others,  $\exp(-b_s k_f S)$ . Non-separability of  $S$  did not allow us to formally solve the two integral equations for a non-trivial solution for  $\chi_1$  and  $\chi_2$  as in ref. [3] and we had to pre-specify a form for  $\chi_2(\mathbf{R}_2)$  in eq.(17) and of  $\chi_1(\mathbf{R}_1)$  in eq.(20). (As long as all the functions, including the meson wave functions and the gluonic field overlap factor  $f$ , are separate in  $\mathbf{R}_1$  and  $\mathbf{R}_2$ , we can everywhere replace  $\chi_1$  and  $\chi_2$  by their analytical integrals which themselves simply multiply if  $\chi_1$  and  $\chi_2$  do, can solve the resulting linear equations for these integrals and can write the  $T$  matrices and phase shifts directly in terms of these integrals. This is what is done in ref.[3][16], but it is hard to think how to generalize this very specialized technique to a case like us where the  $f$  factor is not separable in  $\mathbf{R}_1$  and  $\mathbf{R}_2$ .) Compelled to use, thus, Born approximation (something already in use [1] for meson-meson scattering; our numerical results mentioned below also justify its use here) for this we used the solutions of eqs.(17) and (20) in absence of interactions (say by letting  $k_f$  approach to infinity, meaning  $f = 0$ ) for  $\chi_1(\mathbf{R}_1)$  and  $\chi_2(\mathbf{R}_2)$ . We chose the coefficient of these plane wave solutions so as to make  $\chi_1(\mathbf{R}_1)$  as Fourier transform of  $\delta(P_1 - P_c(1))/P_c^2(1)$  and  $\chi_2(\mathbf{R}_2)$  as Fourier transform of  $\delta(P_2 - P_c(2))/P_c^2(2)$ , with  $P_c(1)$  and  $P_c(2)$  defined below just after eq.(26). Thus we used

$$\chi_2(\mathbf{R}_2) = \sqrt{\frac{2}{\pi}} \exp(i\mathbf{P}_2 \cdot \mathbf{R}_2) \quad (21)$$

inside the integral to get one equation (after a Fourier transform with respect to  $R_1$  and kernel  $e^{i\mathbf{P}_1 \cdot \mathbf{R}_1}$ ) as

$$\begin{aligned} \left(3\omega + \frac{P_1^2}{2\mu_{12}} - E_C\right) \chi_1(\mathbf{P}_1) = & \\ & -\sqrt{\frac{2}{\pi}} \frac{1}{(2\pi)^{\frac{3}{2}}} \int d^3 R_1 d^3 R_2 d^3 R_3 \exp \left\{ i(\mathbf{P}_1 \cdot \mathbf{R}_1 + \mathbf{P}_2 \cdot \mathbf{R}_2) \right\} \\ & \exp \left( -b_s k_f S \right) \exp \left( -\frac{R_1^2 + R_2^2 + 2R_3^2}{2d^2} \right) \\ & \left[ -\frac{8}{6m(2\pi d^2)^3} g_1 + \frac{32}{9(2\pi d^2)^3} \left( -4CR_3^2 - 2\overline{C} \right) - \frac{8(E_C - 4m)}{3(2\pi d^2)^3} \right], \quad (22) \end{aligned}$$

with  $\chi_1(\mathbf{P}_1)$  being Fourier transform of  $\chi_1(\mathbf{R}_1)$ . The formal solution [3] of eq.(22) can be written as

$$\begin{aligned} \chi_1(\mathbf{P}_1) = & \frac{\delta(P_1 - P_c(1))}{P_c^2(1)} - \frac{1}{\Delta_1(P_1)} \frac{1}{16\pi^5 d^6} \int d^3 R_1 d^3 R_2 d^3 R_3 \exp \left\{ i(\mathbf{P}_1 \cdot \mathbf{R}_1 + \mathbf{P}_2 \cdot \mathbf{R}_2) \right\} \\ & \exp \left( -b_s k_f S \right) \exp \left( -\frac{R_1^2 + R_2^2 + 2R_3^2}{2d^2} \right) \left[ -\frac{8}{6m} g_1 + \frac{32}{9} \left( -4CR_3^2 - 2\overline{C} \right) - \frac{8}{3} (E_C - 4m) \right], \quad (23) \end{aligned}$$

with

$$\Delta_1(P_1) = \frac{P_1^2}{2\mu_{12}} + 3\omega - E_c - i\varepsilon.$$

If we choose  $x$ -axis along  $\mathbf{P}_1$  and choose  $z$ -axis in such a way that  $xz$ -plane becomes the plane containing  $\mathbf{P}_1$  and  $\mathbf{P}_2$ , the above equation becomes

$$\chi_1(\mathbf{P}_1) = \frac{\delta(P_1 - P_c(1))}{P_c^2(1)} - \frac{1}{\Delta_1(P_1)} F_1, \quad (24)$$

where, in the notation of eq.(15),

$$F_1 = \frac{1}{16\pi^5 d^6} \int_{-\infty}^{\infty} dx_1 dx_2 dx_3 dy_1 dy_2 dy_3 dz_1 dz_2 dz_3 \exp \left\{ iP(x_1 + x_2 \cos \theta + z_2 \sin \theta) \right\} \exp \left( -b_s k_f S \right) \exp \left\{ -\frac{x_1^2 + y_1^2 + z_1^2 + x_2^2 + y_2^2 + z_2^2 + 2(x_3^2 + y_3^2 + z_3^2)}{2d^2} \right\} \left[ -\frac{8}{6m} g_1 + \frac{32}{9} \left\{ -4C(x_3^2 + y_3^2 + z_3^2) - 2\bar{C} \right\} - \frac{8}{3} (E_C - 4m) \right]. \quad (25)$$

Here  $\theta$  is the angle between  $\mathbf{P}_2$  and  $\mathbf{P}_1$  and because of elastic scattering  $P_1 = P_2 = P$ . From eq.(24) we can write, as in ref. [3], the 1, 2 element of the T-matrix as

$$T_{12} = 2\mu_{12} \frac{\pi}{2} P_c F_1. \quad (26)$$

Here  $P_c = P_c(2) = P_c(1) = \sqrt{2\mu_{12}(E_c - (M_1 + M_2))}$  and  $M_1 = M_2 = 3\omega/2$ ; see paragraph after eq.(19). Using the relation

$$s = I - 2iT = \exp(2i\Delta)$$

or

$$\begin{pmatrix} 1 & 0 \\ 0 & 1 \end{pmatrix} - 2i \begin{pmatrix} T_{11} & T_{12} \\ T_{21} & T_{22} \end{pmatrix} = \begin{pmatrix} 1 & 0 \\ 0 & 1 \end{pmatrix} + 2i \begin{pmatrix} \delta_{11} & \delta_{12} \\ \delta_{21} & \delta_{22} \end{pmatrix}$$

between  $s$  matrix and the  $T$  matrix (actually in the form of elements  $\delta_{ij} = -T_{ij}$  for  $i, j = 1, 2$ ) we got different results for phase shifts for different values of center of mass kinetic energy  $T_c$  and the angle  $\theta$  between  $\mathbf{P}_1$  and  $\mathbf{P}_2$ ; we have used the Born approximation to neglect higher powers in the exponential series. We also probed different values of the parameter  $k_f$ .

For a comparison, we also did the much less time consuming (but approximate) calculation using  $S_a$  in place of  $S$  in eq.(22). This allowed us separating the 9 variables dependence of the integrand as a product, resulting in three triple integrals to be only multiplied, making the convergence very fast in the numerical computation of the integral. Thus we had instead

$$\chi_1(\mathbf{P}_1) = \frac{\delta(P_1 - P_c(1))}{P_c^2(1)} - \frac{1}{\Delta_1(P_1)} F, \quad \text{with} \quad (27)$$

$$F = \frac{1}{16\pi^5 d^6} \left[ \int_{-\infty}^{\infty} dx_1 dx_2 dx_3 \left\{ f_1(x_1, x_2, x_3) \exp \left[ -\frac{x_1^2 + x_2^2 + 2x_3^2}{2d^2} \right] - b_s k_f \left( ax_1^2 + dx_1 x_2 + jx_1 x_3 + bx_2^2 + gx_2 x_3 + cx_3^2 \right) + iP(x_1 + x_2 \cos \theta) \right\} Q(y) \times Q(z) + \int_{-\infty}^{\infty} dy_1 dy_2 dy_3 \left\{ f_2(y_1, y_2, y_3) \exp \left[ -\frac{y_1^2 + y_2^2 + 2y_3^2}{2d^2} \right] - b_s k_f \left( ay_1^2 + ey_1 y_2 + ky_1 y_3 + by_2^2 + hy_2 y_3 + cy_3^2 \right) \right\} Q(x) \times Q(z) + \int_{-\infty}^{\infty} dz_1 dz_2 dz_3 \left\{ f_3(z_1, z_2, z_3) \exp \left[ -\frac{z_1^2 + z_2^2 + 2z_3^2}{2d^2} \right] - b_s k_f \left( az_1^2 + fz_1 z_2 + lz_1 z_3 + bz_2^2 + iz_2 z_3 + cz_3^2 \right) + iPz_2 \sin \theta \right\} Q(x) \times Q(y) \right]. \quad (28)$$

Here

$$f_1(x_1, x_2, x_3) = -\frac{8}{6m} \left( -1.4417 + 0.0258x_1^2 + 0.0254x_2^2 - 4.1914 \times 10^{-7} x_1 x_3 + 0.0258x_3^2 \right) + \frac{32}{9} \left( -4Cx_3^2 - 2\bar{C} \right) - \frac{8}{3} (E_c - 4m),$$

$$\begin{aligned}
f_2(y_1, y_2, y_3) &= -\frac{8}{6m} \left( 0.0258y_1^2 + 0.0254y_2^2 - 4.1914 \times 10^{-7}y_1y_3 + 0.0258y_3^2 \right) - \frac{128}{9}Cy_3^2, \\
f_3(z_1, z_2, z_3) &= -\frac{8}{6m} \left( 0.0258z_1^2 + 0.0254z_2^2 + 5.1396 \times 10^{-6}z_1z_3 + 0.0258z_3^2 \right) - \frac{128}{9}Cz_3^2, \\
Q(x) &= \int_{-\infty}^{\infty} dx_1 dx_2 dx_3 \exp \left[ -\frac{x_1^2 + x_2^2 + 2x_3^2}{2d^2} - b_s k_f \left( ax_1^2 + dx_1x_2 + jx_1x_3 + bx_2^2 + gx_2x_3 + cx_3^2 \right) + \right. \\
&\quad \left. iP(x_1 + x_2 \cos \theta) \right], \\
Q(y) &= \int_{-\infty}^{\infty} dy_1 dy_2 dy_3 \exp \left[ -\frac{y_1^2 + y_2^2 + 2y_3^2}{2d^2} - b_s k_f \left( ay_1^2 + ey_1y_2 + ky_1y_3 + by_2^2 + hy_2y_3 + cy_3^2 \right) \right] \\
Q(z) &= \int_{-\infty}^{\infty} dz_1 dz_2 dz_3 \exp \left[ -\frac{z_1^2 + z_2^2 + 2z_3^2}{2d^2} - b_s k_f \left( az_1^2 + fz_1z_2 + lz_1z_3 + bz_2^2 + iz_2z_3 + cz_3^2 \right) + iPz_2 \sin \theta \right].
\end{aligned}$$

For this choice of  $S$ , we also calculated the phase shifts that are reported in the next section. By treating eq.(20) in the same fashion as that of eq.(17) and using the Born approximation

$$\chi_1(\mathbf{R}_1) = \sqrt{\frac{2}{\pi}} \exp(i\mathbf{P}_1 \cdot \mathbf{R}_1) \quad (29)$$

it was checked that the results for phase shifts remain same. Actually eq.(20) and eq.(17) become identical if we interchange  $\mathbf{R}_1$  and  $\mathbf{R}_2$ .

## 5 Results and conclusion

Fig.1 shows our results, with  $k_f$  defined by eq.(11) taken as 0.5, for the phase shifts for a selection of center of mass kinetic energies for different angles between  $\mathbf{P}_1$  and  $\mathbf{P}_2$  (Some numerical uncertainty appears at 0.15GeV for  $\theta = 0$ . When we further explored the region between 0.14GeV and 0.16GeV there appeared fluctuations in the results. For smoothness in graph we have neglected the data point at 0.15GeV in fig.1 at  $\theta = 0$  and interpolated data points are taken there.)

We found no numerical fluctuations for kinetic energies above 0.16GeV, and thus we conclude that in this kinematical range the scattering angle has large effect on phase shifts, indicating a true gluonic field effect. (The origin of this angle dependence is the exponent  $S$  which is essentially in a model of  $W_{12}$  Wilson loop, a pure gluonic theory expectation value; we do not get any angle dependence if this  $S$  is not used. So the angle dependence emerges from gluonic field related to the area law, and is thus a QCD effect.) By increasing the scattering angle the phase shifts become large. We noted that a faster convergence of the nine-dimensional integration (see eq.(25)) for large kinetic energy values was possible for smaller values of the parameter  $k_f$ ; for a decrease in  $k_f$  of 0.1 the CPU time reduced at least three times to that for the previous value. Thus we used the smaller value of  $k_f = 0.5$  mentioned in ref.[4] to get phase shifts for a larger set of kinetic energies resulting in smoother graphs. For the above mentioned value  $C = -0.0249281\text{GeV}^3$  (meaning  $\omega = 0.665707\text{GeV}$  and  $d = 0.441357$  fm) used in ref.[14] (giving the 99.4% overlap of the wave functions) we found that, at  $T_c = 0.1\text{GeV}$ , there is about a 1 degree change in phase shift for a 30 degree change in scattering angle  $\theta$ , even larger in magnitude than the phase shifts of fig.1 for the corresponding  $T_c$  given by our routine value  $d = 0.556$  fm. So we can say that the characteristic feature of angle dependence will remain if we study the scattering of some realistic meson meson system by taking sizes of mesons accordingly and adjust the parameters of the Gaussian wave functions to simulate realistic linear plus Columbic potential eigenfunctions.

For a comparison with the other crude forms of  $f$  previously used, we show in the following fig.2 the average of these  $k_f = 0.5$  phase shifts over our selection of angle  $\theta$  values along with the corresponding phase shifts for other forms of  $f$  i.e. exponent in  $f$  being proportional to  $S_a$ ,  $\sum_{i < j} r_{ij}^2$  and zero; the phase shifts were found to be independent of the angle  $\theta$  for all these older forms of  $f$  and hence there was no need to take any angle-average for these other forms. This figure shows that in comparison to  $k_f = 0$  (sum of two body potential model) we get relatively very small coupling with  $S$ ,  $S_a$  and Gaussian form in  $f$ . The introduction of a many-body interaction in the previous (Gaussian) form of  $f$  resulted in a reduced meson-meson interaction. In ref. [3] this reduction was noted as decreased meson-meson phase shifts. So there are less chances of making a bound state with modifications in sum of two body approach i.e. the inclusion of gluonic field effects significantly decrease coupling between two mesons in a  $q^2\bar{q}^2$  system. Phase shifts are much less than 1 radian which indicates the validity of Born approximation. The phase shifts we get are lesser than reported by others who have used Born approximation [1] but not used  $f$  factor in off-diagonal terms.

It is to be noted that the  $S_a$  form also does not result in any angle dependence, although in contrast to the  $f = 1$  and Gaussian form there is apparently no a priori reason to expect such an angle independence for the use of  $S_a$ . This may be because  $S_a$  is almost Gaussian with a little mixture of  $x_1x_3$  and  $z_1z_3$  terms (see eq.(16) and the parameter values reported just below it) or because  $S_a$  can be converted to a Gaussian form by a completing of squares. As for a comparison of the  $S_a$  phase shifts with the angle-average of the  $S$  phase shifts, it can be pointed out that the height of phase shift with  $S_a$  became less than that with original  $S$  but the shape remains identical. Perhaps this indicates that  $S_a$  simulates well some variations resulting from the original  $S$  form. In fig.2, if we compare graph of Gaussian form with the angle averaged phase shifts using  $S$  in  $f$  we find that as compared to Gaussian form the graph of other forms is closer to  $k_f = 0$ , though the height of graph with  $k_f = 0$  is still very large as compared to both Gaussian form of  $f$  and that of  $S$  in  $f$ ; see fig.7 which clarifies any ambiguity, if so, in fig.2 about the  $k_f=0$  results.

Fig.3 reports most of the results for the higher values 0.57 of  $k_f$  mentioned in ref. [4]. This value is more precise for their form of model and the crude area expression in the exponent in it. But our numerical calculations for this value turned out to be more demanding and thus were done for a smaller selection of kinetic energies. The numerical uncertainties for this value are for  $\theta = \frac{\pi}{2}$  and the kinetic energy between 0.11GeV and 0.12GeV; the results for this value of  $\theta$  are in fig.5.

A value of  $k_f = 1.0$  higher than 0.5 and 0.57 mentioned above has been reported in ref. [24]. Although this work analyzes a relatively limited collection of geometries (only squares and tilted rectangles), we have tried to see effects of using a higher  $k_f$ . The numerical problems for large  $k_f$  implied in the above mentioned numerical convenience for smaller  $k_f$  did not allow us to get results for  $k_f=1$  in a manageable time even for  $T_c = 0.1\text{GeV}$ . The best we could do was to do a number of calculations for  $k_f = 0.8$ ; the resulting phase shifts from these are shown in fig.4 except for the phase shifts for  $\theta = \pi/2$  that are reported in fig.6, showing some numerical uncertainties at the kinetic energy=0.13GeV and at 0.49–0.51GeV. Based on fig.4 and fig.6, we expect that for higher values of  $k_f$  the results will remain qualitatively same and do not expect any new feature to emerge for  $k_f = 1$ .

We did a partial wave analysis for the phase shifts in fig. 1. For this we have projected our angle dependence on  $m = 0$  spherical harmonics. The angle dependence is independent of azimuthal angle  $\phi$  so the partial wave expansion will only contain terms independent of angle  $\phi$  or terms with  $m=0$ . This analysis shows that below 0.2GeV the S-wave is very much dominant as can be seen by a sharp rise of graphs towards lower side in fig. 8 and fig. 9 near 0.2GeV and it is also justified from fig. 1 which shows a  $\theta$  independence below 0.2GeV i.e. purely an S-wave. Our partial wave analysis shows that only even partial waves are present. Furthermore partial wave phase shifts decrease as we go from S-wave to I-wave, as is clear from large reciprocals in fig. 9, and they become negligible as compared to corresponding S-wave phase shifts as we go beyond G-wave. So here in figs. (8,9) only S/D and S/G ratios are plotted. The reason for the absence of odd partial waves is that our phase shifts are symmetric around  $\theta = \frac{\pi}{2}$  and the product of an even and odd function is an odd function giving rise to a zero result after integration. Thus phase shift is different for different angle and partial wave analysis of this angle dependence indicates presence of  $l = 2, 4$  spherical harmonics along with the angle independent  $l = 0$ . We have found this extra presence of D, G waves in angle dependence only when we use  $e^{-\text{constant*area}}$  form of  $f$ . But when  $f$  is spherically symmetric, i.e. old Gaussian form, then there appears no D, G waves. Thus D, G waves must be a property of  $e^{-\text{constant*area}}$ . So  $e^{-\text{constant*area}}$  may couple an  $l=0$  meson-meson system to  $l=2, 4, \dots$  etc. systems. This means two possibilities 1)  $l=0$  meson-meson system may have t-matrix and phase shifts to  $l=2, 4, \dots$  final state meson-meson systems and 2)  $l=0$  may couple to  $l=2, 4, \dots$  states as intermediate states in a polarization potential [19], through  $e^{-\text{constant*area}}$ .

## Acknowledgments

We are thankful to Higher Education Commission (HEC) of Pakistan for there financial support through Grant No. 17-5-3(Ps3-056) HEC/Sch/2006.

## References

- [1] T. Barnes and E.S. Swanson, Phys.Rev. **D46** 131-159 (1992).
- [2] A. M. Green, C. Michael, J.E. Paton, Nucl.Phys. **A554** 701-720 (1993).

- [3] B. Masud, J.Paton, A.M. Green and G.Q. Liu, Nucl.phys. **A528** 477-512 (1991).
- [4] A.M. Green and P. Pennanen, Phys.Rev. **C57** 3384-3391 (1998).
- [5] H. Matsuoka, D. Sivers, Phys.Rev. **D33** 1441 (1986).
- [6] A. M. Green, J. Koponen and P. Pennanen, Phys.Rev. **D61** 014014, (1999).
- [7] V. G. Bornyakov, P. Yu. Boyko, M. N. Chernodub and M. I. Polikarpov, arXiv:hep-lat/0508006v1.
- [8] Hideo Suganuma, Arata Yamamoto, Naoyuki Sakumichi, Toru T. Takahashi, Hideaki Iida and Fumiko Okiharu, Mod. Phys. Lett. **A23** 2331 (2008).
- [9] J. Vijande, A. Valcarce and J. M. Richard, Phys.Rev. **D76** 114013 (2007).
- [10] J. Weinstein and N. Isgur, Phys.Rev.**D27** 588-599 (1983).
- [11] B. Silvestre-Brac and C. Semay, Z.Phys. **C57** 273-282 (1993).
- [12] E.S. Swanson, Ann.Phys. (N.Y.) 220,73 (1992).
- [13] John Archibald Wheeler, Phys.Rev. **52** 1083 (1937).
- [14] E. S. Ackleh, T. Barnes and E. S. Swanson, Phys. Rev. **D54** 6811 (1996).
- [15] C. Alexandrou, T. Karapiperis, O. Morimatsu, Nucl.Phys. **A518** 723-751 (1990).
- [16] B. Masud , Phys. Rev. **D50** 6783-6803 (1994).
- [17] P. Bicudo and M. Cardoso, arXiv:1010.0281.
- [18] Fumiko Okiharu, Hideo Suganuma and Toru T. Takahashi, Phys.Rev. **D72** 014505 (2005).
- [19] Cheuk-Yin Wong, Phys.Rev. **C69** 055202 (2004), arXiv:hep-ph/0311088v2.
- [20] M. Imran Jamil and Bilal Masud, in progress.
- [21] J. Weinstein and N. Isgur, Phys.Rev. **D41** 2236 (1990).
- [22] N. Isgur and J. Paton, Phys.Rev. **D31** 2910 (1985).
- [23] M. Teper, Phys. Lett. **B397** 223 (1997).
- [24] Petrus Pennanen, Phys.Rev. **D55** 3958 (1997).
- [25] S. Furui, A.M. Green and B. Masud, Nucl.Phys **A582** 682-696 (1995).
- [26] D. Ahmad and B. Masud, in progress.

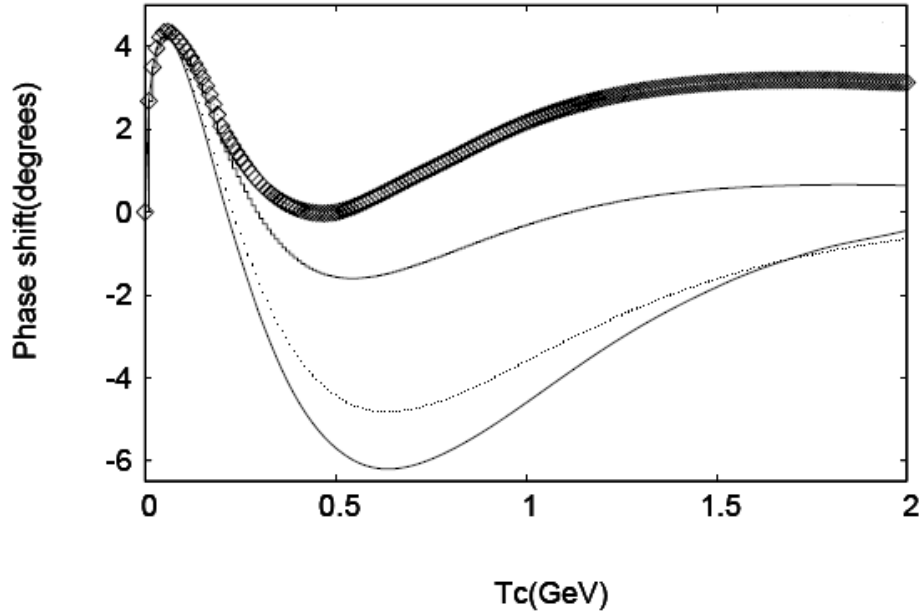


Figure 1: For  $k_f = 0.5$ , the comparison of phase shifts for different values of  $\theta$  using  $S$  in  $f$ . The graph with points is for  $\theta = 0$ , with steps for  $\theta = \frac{\pi}{6}$  and with dots only is for  $\theta = \frac{\pi}{3}$ . The graph with lines is for  $\theta = \frac{\pi}{2}$ ; here the data is equally spaced as in the other graphs but data points are joined.

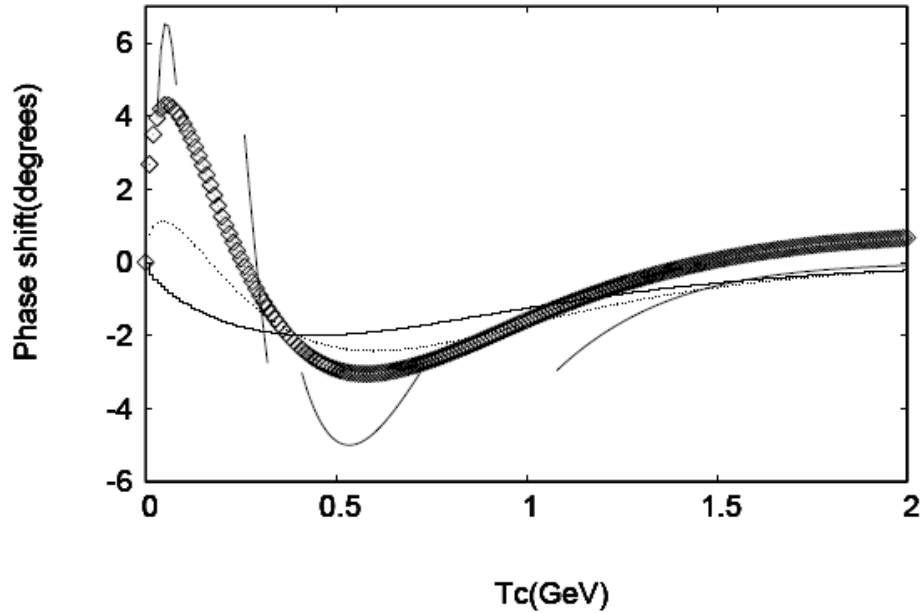


Figure 2: Comparison of different forms of  $f$ . Graph with lines only corresponds to  $k_f = 0$ . (Here data points are 0.01GeV apart but they are joined for clarity. This graph is also shown separately in fig.7. Only four portions of the graph are shown here: upper peak corresponds to actual data minus 28 and lower peak corresponds to actual data plus 5.) Graph with dots corresponds to  $S_a$  in  $f$ . Graph with steps corresponds to gaussian form of  $f$  for  $k_f = 0.075$  as defined by eq.(12). Graph with points corresponds to average of phase shifts for different values of angle  $\theta$  for  $S$  in  $f$  with  $k_f = 0.5$  defined by eq.(11).

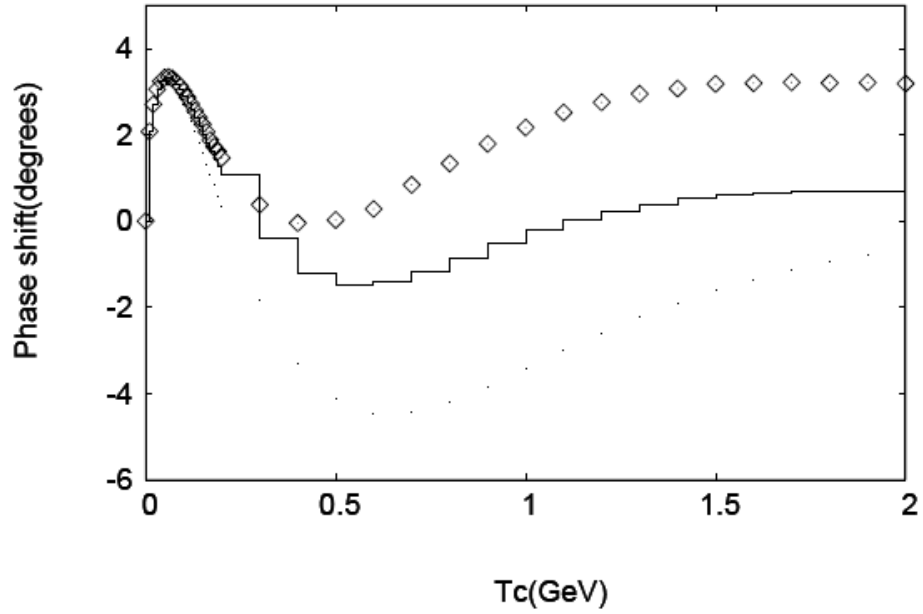


Figure 3: Comparison of phase shifts for different values of  $\theta$  using  $S$  in  $f$  with  $k_f = 0.57$ . Choice of curve shapes is same as in fig. 1. But the results for  $\theta = \pi/2$  are shown in fig. 5 and not here.

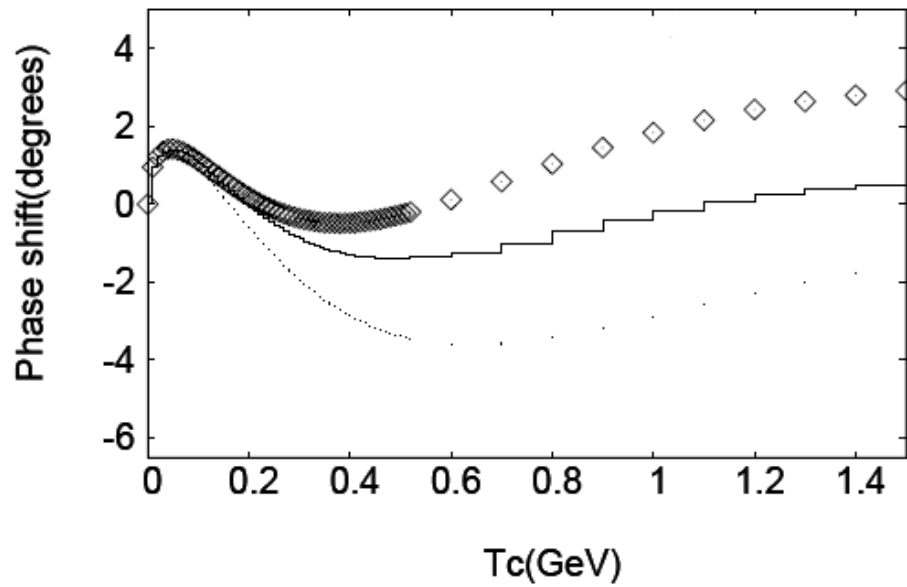


Figure 4: Comparison of phase shifts for different values of  $\theta$  using  $S$  in  $f$  with  $k_f = 0.8$ . Choice of curve shapes is same as in fig. 3. The results for  $\theta = \pi/2$  are shown in fig. 6 below.

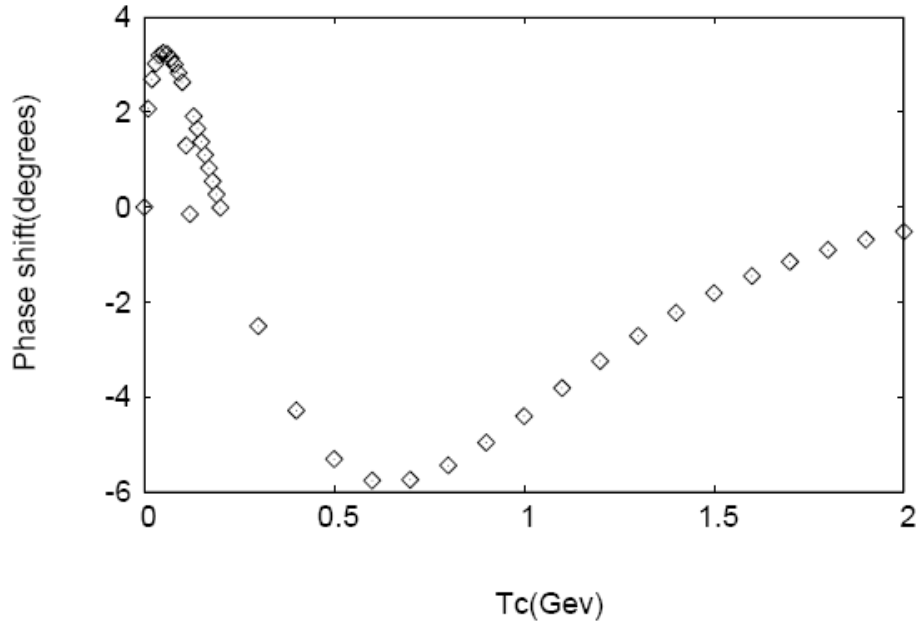


Figure 5: Phase shifts for  $k_f = 0.57$  at  $\theta = \frac{\pi}{2}$  using  $S$  in  $f$ .

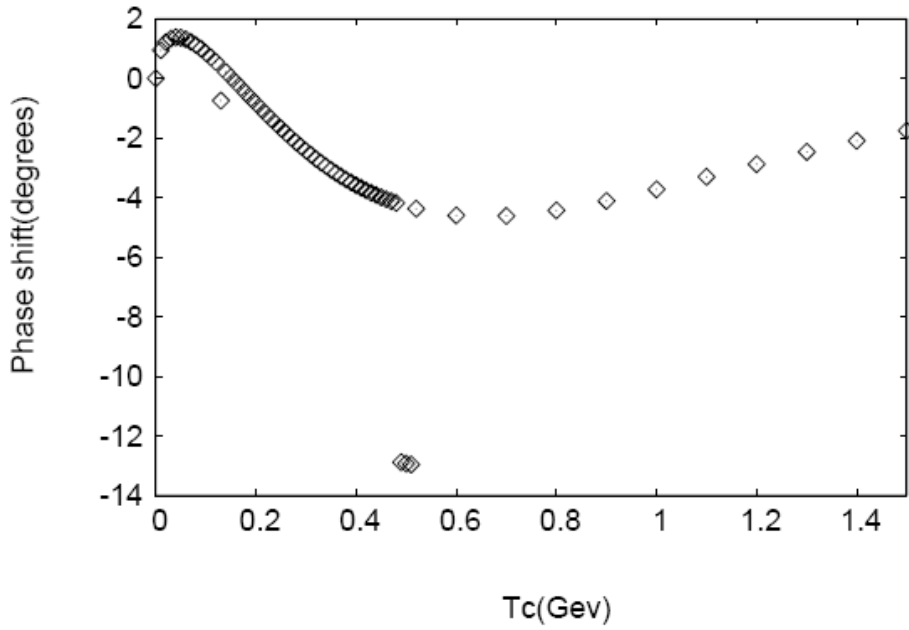


Figure 6: Phase shifts for  $k_f = 0.8$  at  $\theta = \frac{\pi}{2}$  using  $S$  in  $f$ .



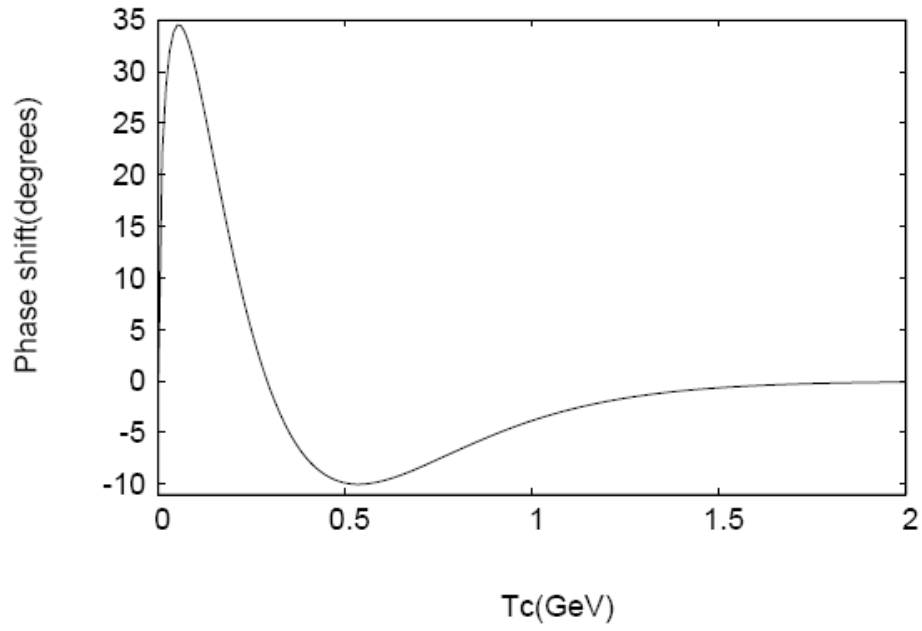


Figure 7: Phase shifts for  $k_f = 0$ .

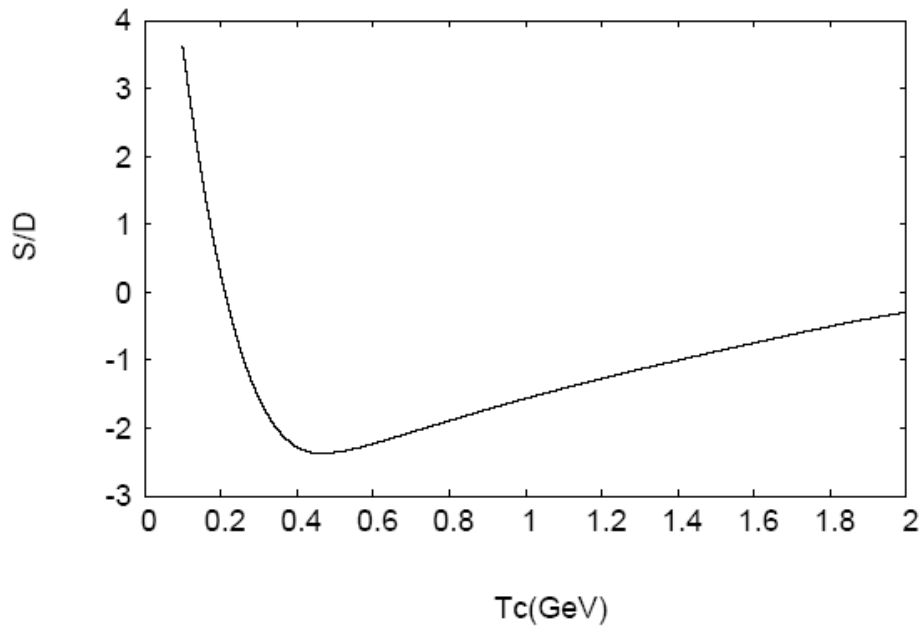


Figure 8: S/D ratios for different values of  $T_c$ .

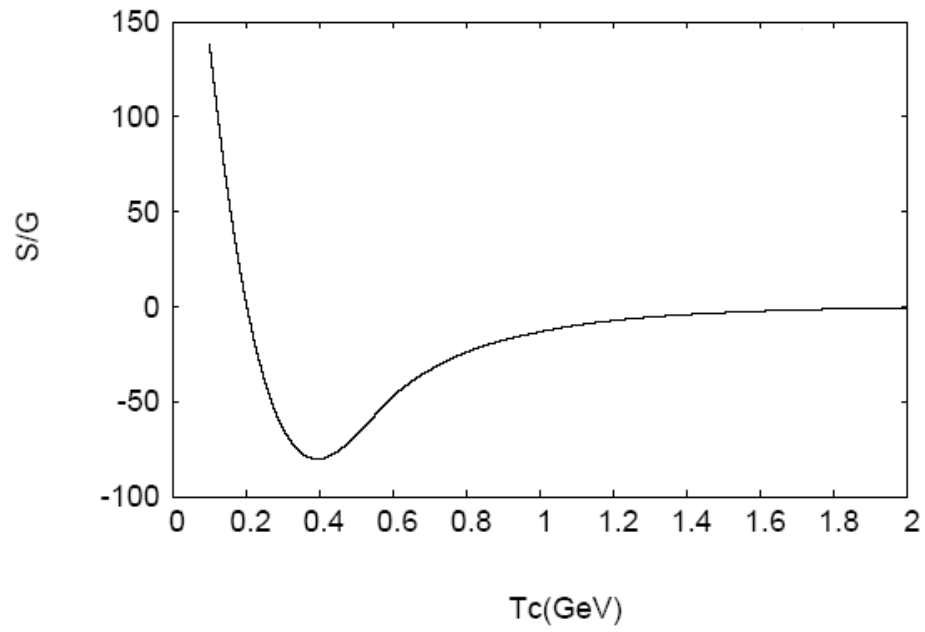


Figure 9: S/G ratios for different values of  $T_c$ .